ENVIRONMENTAL ENGINEERING SCIENCE
Volume 24, Number 1, 2007


# Kinetic Study for Photocatalytic Oxidation of Elemental Mercury on a $SiO_2$–$TiO_2$ Nanocomposite

**Ying Li and Chang-Yu Wu***

*Department of Environmental Engineering Sciences*
*University of Florida*
*Gainesville, FL 32611-6450*

## ABSTRACT

The kinetics of photocatalytic oxidation of elemental mercury ($Hg^0$) on a $SiO_2$–$TiO_2$ nanocomposite with UV irradiation was studied in a fix-bed reactor under both dry and humid conditions. The experimental data were analyzed using a Langmuir-Hinshelwood (L-H) model. The reaction rate was successfully expressed using the model, indicating the L-H nature of $Hg^0$ photocatalytic oxidation on the $SiO_2$–$TiO_2$ nanocomposite. The L-H model prediction suggests a great potential of the $SiO_2$–$TiO_2$ nanocomposite for $Hg^0$ removal from high concentration emission sources. On the other hand, the rate of photocatalytic $Hg^0$ oxidation was found to be significantly inhibited by the presence of water vapor. This may be explained by the competitive adsorption of water vapor on the $TiO_2$ surface, which results in the reduction of available adsorption sites for $Hg^0$.

**Key words:** photocatalytic oxidation; kinetics; mercury; water vapor; $SiO_2$–$TiO_2$ nanocomposite

## INTRODUCTION

Mercury (Hg) is listed as one of the hazardous air pollutants (HAPs) in the 1990 Clean Air Act Amendments (CAAA). In the ecosystem, Hg tends to bioaccumulate in the food chain, thus exerting significant impacts on human health (Brown *et al*., 1999). The major sources of anthropogenic Hg emissions in the United States are coal combustors (U.S. EPA, 1997). Consequently, in 2005, the U.S. EPA (2005) issued the Clean Air Mercury Rule to permanently cap and reduce mercury emissions from coal-fired power plants.

Many methodologies have been proposed for Hg emission control. Among them, the technology of sorbent injection, particularly activated carbon injection, has been investigated most intensively. This technology has been successfully implemented in the municipal waste incinerator industry, where 90% Hg removal can be achieved (Pavlish *et al*., 2003). However, the application of sorbent injection in coal-fired utility boilers is far more challenging due to the shorter gas residence time, the lower equilibrium adsorption capacity and mass-transfer rate, and the compromise of fly ash properties by the injected sorbent (Pavlish *et al*., 2003). A novel methodology using titanium dioxide ($TiO_2$)-based nanostructured sorbents has been demonstrated to be very effective for capture of elemental mercury ($Hg^0$) under ultraviolet (UV) irradiation (Wu *et al*., 1998; Lee *et al*., 2001; Pitoniak *et*

*Corresponding author: Department of Environmental Engineering Sciences, University of Florida, P.O. Box 116450, Gainesville, FL 32611-6450. *Phone:* 352-392-0845; *Fax:* 352-392-3076; *E-mail:* cywu@ufl.edu

*al*., 2003). Wu *et al.* (1998) and Lee *et al.* (2001) reported a high level of $Hg^0$ capture in simulated combustor exhaust using *in situ* generated $TiO_2$ particles, while Pitoniak *et al.* (2003) used a highly porous silica ($SiO_2$) gel doped with $TiO_2$ nanoparticles and achieved synergistic adsorption and photocatalytic oxidation of $Hg^0$ in a fixed-bed reactor. The high surface area and open structure of the $SiO_2$–$TiO_2$ nanocomposite allow effective irradiation by UV light, and thus minimize the mass-transfer resistance for $Hg^0$ (Wu *et al*., 1998; Pitoniak *et al*., 2003).

To make an effective design of the photocatalytic reactor, a solid understanding of the reaction kinetics is of great importance. Lee *et al.* (2004) studied $Hg^0$ oxidation by $TiO_2$ nanoparticles with UV irradiation in a differential bed reactor (DBR) and an aerosol flow reactor (AFR), and correlated the overall reaction rate with the initial $Hg^0$ concentration and UV intensity. However, the kinetic parameters on water vapor dependence were not available in that study, while water vapor is an important component in the flue gas and plays a critical role in the chemistry of mercury in coal-fired boilers (Edwards *et al*., 2001; Niksa *et al*., 2001). Rodríguez *et al.* (2004) developed a mechanistic model to predict $Hg^0$ capture with *in situ*-generated $TiO_2$ nanoparticles by solving the equilibrium equations for electron-hole pair generation/consumption. They also compared their mechanistic model with the Langmuir-Hinshelwood (L-H) model used by Obee (1996) for characterizing photocatalytic oxidation of certain organic compounds. At low water vapor concentrations, the Hg capture rate predicted by the mechanistic model (Rodriguez *et al*., 2004) was proportional to the square root of the water vapor concentration, whereas the L-H model (Obee, 1996) indicated first-order dependence. At high water vapor concentrations, both models predicted a constant Hg capture rate that was independent of the water vapor concentration.

Some other modeling studies have been done on Hg capture using activated carbon. Rostam-Abadi *et al.* (1997) applied an empirical equation to the mass balance for $Hg^0$ sorption on carbon particles in a duct flow reactor and derived the minimum C/Hg ratio required to reduce $Hg^0$ at a certain inlet $Hg^0$ concentration. Chen *et al.* (1996) derived an equation to model mercury capture when it is limited by both mass transfer and capacity by assuming that adsorption at the surface obeys Henry's law. A conceptually similar approach was used by Flora *et al.* (1998) based on the Langmuir isotherm and by Meserole *et al.* (2000) based on the Freundlich equation. Several other studies (Kim and Hong, 2002; Shang *et al*., 2002; Raillard *et al*., 2004; Son *et al*., 2004) have been conducted on photocatalytic oxidation of various volatile organic compounds (VOCs) by $TiO_2$, and the experimental data matched well with the L-H kinetic model. This intriguing L-H nature of a wide range of VOCs warrants the investigation on the correlation between the kinetics of $Hg^0$ photocatalytic oxidation by $TiO_2$ and the L-H rate expression, whereas no relevant research has been done so far. In addition, the L-H model takes advantages over the other models previously described in incorporating the effect of competitive adsorption of water vapor. Therefore, the purpose of this research was to study the kinetics of the $Hg^0$ photocatalytic oxidation on a $SiO_2$–$TiO_2$ nanocomposite by using the L-H model to analyze the kinetic data. The role of water vapor in $Hg^0$ photocatalytic oxidation was established as well. This kinetic modeling study is of importance in predicting $Hg^0$ removal efficiency and is useful for designing an effective reactor, under photocatalyzed oxidizing conditions.

## MATERIALS AND METHODS

### *Synthesis of $SiO_2$–$TiO_2$ nanocomposite*

The $SiO_2$–$TiO_2$ nanocomposite was synthesized following a sol-gel method (Pitoniak *et al.*, 2003) using deionized water, ethanol, tetraethyl orthosilicate (TEOS) with $HNO_3$, and HF added as catalysts to increase the hydrolysis and condensation rates. First, the chemicals were added to a polymethylpentene container, and then $TiO_2$ nanoparticles (Deggusa, P25) were added to the batch with a magnetic stir plate providing sufficient mixing. After that, the solution suspended with $TiO_2$ nanoparticles was pipetted into polystyrene 96-well assay plates before the gelation occurred. The pellets were later aged at room temperature for 2 days and then at 65°C for another 2 days. After aging, the pellets were removed from the plates, rinsed with deionized water to remove any residual acid or ethanol. Next, the pellets were placed in a programmable oven and heated at 103°C for 18 h to remove any residues of liquid solution within the silica network and then at 180°C for 6 h to harden the gel. Finally, the temperature was slowly decreased back to room temperature over a 90-min period. The final size of an individual cylindrical pellet was approximately 5 mm in length and 3 mm in diameter. The loading of $TiO_2$ in the nanocomposite was 12 wt%, which corresponded to the optimum performance of $Hg^0$ removal using the $SiO_2$–$TiO_2$ nanocomposite (Pitoniak *et al*., 2003). The average BET (Brunauer, Emmett, and Teller equation) surface area of the nanocomposite was measured to be 280 $m^2\ g^{-1}$ using a Quantachrome NOVA 1200 Gas Sorption Analyzer (Boynton Beach, FL).

### *Apparatus and procedure*

Figure 1 shows the schematic diagram of the experimental system. An incoming cylinder air was divided into

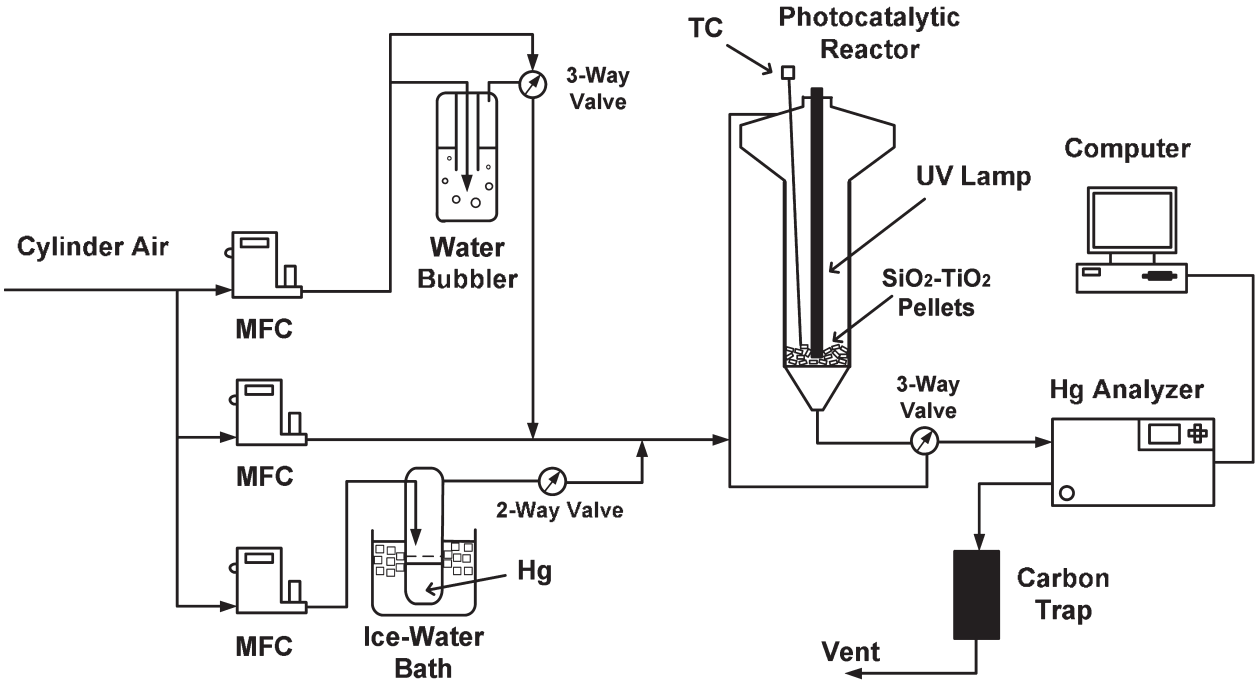


**Figure 1.** Schematic diagram of the experimental system.

three streams, the flow rates of which were controlled by mass flow controllers (MFC, Model. FMA 5400/5500, Omega Engineering, Inc., Stamford, CT). The total flow rate remained constant at 2 L/min. One of the air streams was allowed to pass through a water bubbler for a humid flow or to bypass it for a dry flow. The second stream served as dilution to adjust the humidity level. The third stream passed through the surface of a liquid $Hg^0$ reservoir and introduced the saturated $Hg^0$ vapor into the system. The $Hg^0$ reservoir was placed in an ice-water bath to maintain a constant $Hg^0$ vapor pressure. Downstream of all the gases was the fixed-bed photocatalytic reactor, the lower part of which is a cylindrical tube of fused quartz 4.5 cm in diameter and 20 cm in length. The reactor was mounted with a fused quartz center with a diameter of 2 cm, which was used to house a UV lamp. The UV light has a peak wavelength of 365 nm with an intensity of 4 mW/cm$^2$ measured by a UVX radiometer (with a UVX-36 sensor probe). At the bottom of the reactor is a glass frit used to hold the $SiO_2$–$TiO_2$ pellets within the bed. A thermocouple (TC, Type K, Omega Engineering, Inc.) was used to monitor the temperature on the surface of the pellets. The $Hg^0$ concentration at the reactor outlet was measured by a RA-915+ Hg analyzer (OhioLumex Co., Cleveland, OH), which is based on Zeeman Atomic Absorption Spectrometry using High-Frequency Modulated light polarization (ZAAS-HFM) (Sholupov *et al*., 2004). The inlet $Hg^0$ concentration was obtained when the $Hg^0$ laden air bypassed the reactor. Finally, the air stream passed through a carbon trap before it was exhausted into the fume hood.

Two sets of experiments were performed in this study. In the first set, no water vapor was introduced into the air stream but with variations in the inlet $Hg^0$ concentration (0.19 to 1.28 $\mu$-mol m$^{-3}$ or 38 to 256 $\mu$g m$^{-3}$). In the second set, the inlet $Hg^0$ concentration remained constant, but with changes in water vapor concentration (0 to 0.95 mol m$^{-3}$). In each experiment, the $Hg^0$ laden air was allowed to pass through the reactor for 1 h to ensure that the $Hg^0$ adsorption on the $SiO_2$–$TiO_2$ nanocomposite reached equilibrium, which was monitored by the online Hg analyzer. Then, the photocatalytic reaction was started by turning on the UV lamp and the $Hg^0$ concentrations were recorded for a certain period of time until no more reduction in $Hg^0$ concentration was observed. All the experiments were conducted under room conditions. In each test, 2.5 g of fresh $SiO_2$–$TiO_2$ pellets were used, which corresponded to an average of 4-mm bed thickness (approximately one single layer of pellets).

## MODEL DESCRIPTION

Photocatalytic oxidation of $Hg^0$ occurs when the $SiO_2$–$TiO_2$ nanocomposite is under UV irradiation as shown in Fig. 2. The hole-electron pairs generated on the

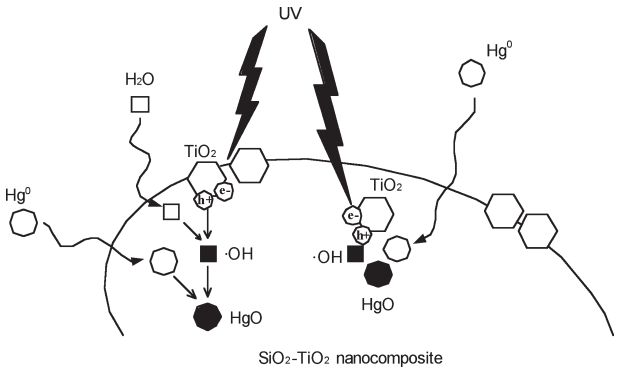


**Figure 2.** Description of $Hg^0$ photocatalytic oxidation on $SiO_2$–$TiO_2$ nanocomposites.

$TiO_2$ particle surfaces lead to the formation of highly reactive hydroxyl (OH) radicals, which are responsible for $Hg^0$ oxidation to form HgO (Wu *et al*., 1998; Pitoniak *et al*., 2003). The mechanism can be described as the following reactions:

$$TiO_2 + hv \rightarrow e^- + h^+ \quad (1)$$

$$H_2O \leftrightarrow H^+ + OH^- \quad (2)$$

$$h^+ + OH^- \rightarrow \cdot OH \quad (3)$$

$$h^+ + H_2O \rightarrow \cdot OH + H^+ \quad (4)$$

$$OH \cdot + Hg^0 \rightarrow HgO \quad (5)$$

Among the factors that affect the efficiency of $Hg^0$ capture by the $SiO_2$–$TiO_2$ nanocomposite, water vapor content in the $Hg^0$ laden air was reported to be one of the most important (Pitoniak *et al*., 2003). On one hand, surface moisture on $TiO_2$ nanoparticles is necessary for generating OH radicals (Reactions 2–4), which are responsible for photocatalytic $Hg^0$ oxidation. On the other hand, at high water vapor concentrations, competitive adsorption may reduce the number of sites available for $Hg^0$ (Pitoniak *et al*., 2003; Rodriguez *et al*., 2004).

Similar to the studies by other researchers (Obee, 1996; Obee and Hay, 1997; Canela *et al*., 1998), the rate of photocatalytic oxidation of $Hg^0$ is defined as

$$r = \frac{(C_{Hg}{}^{in} - C_{Hg}{}^{out}) \times Q}{A_e} \quad (6)$$

where $C_{Hg}{}^{in}$ is the $Hg^0$ concentration at the inlet of the reactor, $C_{Hg}{}^{out}$ is the $Hg^0$ concentration at the outlet of the reactor at steady state, $Q$ is the volumetric flow rate of the $Hg^0$ laden air (2 L $min^{-1}$ or 0.12 $m^3$ $h^{-1}$), and $A_e$ is the effective surface area of the pellets that is exposed to UV light. It should be noted that only a thickness of 0.1 mm from the surface of the pellets and only the areas facing the UV light can effectively contribute to $Hg^0$ oxidation (Pitoniak *et al*., 2005). Thus, $A_e$ can be calculated as

$$A_e = SA \times m \times f_V \times f_P \quad (7)$$

where $SA$ is the specific surface area of the pellets (280 $m^2$ $g^{-1}$), m is the mass of pellets used (2.5 g), $f_V$ is the volume fraction of the 0.1 mm thickness layer that UV light can penetrate (estimated to be 0.15), and $f_P$ is the packing factor that accounts for the fraction of the surface areas exposed to UV light (estimated to be 0.5).

To correlate the experimental data of photocatalytic oxidation rate of $Hg^0$, the L-H rate equation was used. If the concentration of water vapor is constant, the L-H expression can be simplified as

$$r = k \frac{K_{Hg}C_{Hg}}{1 + K_{Hg}C_{Hg}} \quad (8)$$

where $r$ is the reaction rate ($\mu$-mol $m^{-2}$ $h^{-1}$), $k$ is the L-H rate constant ($\mu$-mol $m^{-2}$ $h^{-1}$), $K_{Hg}$ is the Langmuir adsorption constant of $Hg^0$ ($m^3$ $\mu$-$mol^{-1}$), and $C_{Hg}$ is the $Hg^0$ concentration ($\mu$-mol $m^{-3}$). $C_{Hg}$ is normally assigned to be the bulk or inlet concentration, $C_{Hg}{}^{in}$ (Obee, 1996; Obee and Hay, 1997). The inverse of equation (8) gives

$$\frac{1}{r} = \frac{1}{kK_{Hg}} \frac{1}{C_{Hg}} + \frac{1}{k} \quad (9)$$

If the assumed L-H expression is valid for Hg photocatalytic oxidation, a plot of $r^{-1}$ vs. $C_{Hg}{}^{-1}$ should be linear. Subsequently, the values of $k$ and $K_{Hg}$ can be derived from the combination of the intercept and the slope of the linear line. From these values, the photocatalytic $Hg^0$ oxidation rate can be predicted by the L-H model.

Similar to the modeling studies conducted by other researchers on photocatalytic oxidation of organic pollutants (Obee and Hay, 1997; Shang *et al*., 2002), when water vapor is present, the inhibitory effect of water vapor on $Hg^0$ photocatalytic oxidation can be assumed according to the following L-H form

$$r = k \frac{K_{Hg}C_{Hg}}{1 + K_{Hg}C_{Hg} + K_wC_w} \quad (10)$$

where $K_w$ is the Langmuir adsorption constant of water and $C_w$ is the water vapor concentration. The inverse of equation (10) gives

$$\frac{1}{r} = \frac{K_w}{kK_{Hg}C_{Hg}} C_w + \frac{1}{k}\left(1 + \frac{1}{K_{Hg}C_{Hg}}\right) \quad (11)$$

The value of $K_{Hg}$ can be obtained from previous analysis when water vapor is not present. When $C_{Hg}$ remains at a constant level and only $C_w$ varies, a plot of $r^{-1}$ vs. $C_w$ should be linear if it follows the L-H model expression. Then the values of $k$ and $K_w$ can be derived from the plot.

## RESULTS AND DISCUSSION

### *Effect of $Hg^0$ concentration*

Figure 3 shows the outlet $Hg^0$ concentration as a function of UV illumination time at six different inlet levels ranging from 0.19 to 1.28 $\mu$-mol $m^{-3}$ (38 to 256 $\mu$g $m^{-3}$) when water vapor was not present. The outlet $Hg^0$ concentration dropped quickly when UV was first turned on for a few minutes and then gradually leveled off. From 20 to 30 min, no significant change in outlet $Hg^0$ concentration was observed and the pellet surface temperature remained almost constant (42.7 $\pm$ 0.3°C). Therefore, 30 min was taken as the time the system reached steady state. Experiments were repeated three times at each inlet $Hg^0$ concentration level. The average $Hg^0$ removal efficiency ranged from 90 to 95%, but was not an apparent function of the inlet $Hg^0$ concentration.

At each inlet $Hg^0$ concentration level, the photocatalytic oxidation rate $r$ can be calculated from equation (6) and the average value can be obtained. A plot of $r^{-1}$ vs. $C_{Hg}{}^{-1}$ is shown in Fig. 4 and the observed linear relationship indicates that the kinetics of $Hg^0$ photocatalytic oxidation fits the L-H model very well. From equation (9), values of the L-H rate constant $k$ and the Langmuir adsorption constant $K_{Hg}$ were calculated to be $k = 0.024$ $\mu$-mol $m^{-2}$ $h^{-1}$ and $K_{Hg} = 0.094$ $m^3$ $\mu$-$mol^{-1}$. Substituting the values of $k$ and $K_{Hg}$ back into equation (8), the photocatalytic oxidation rates at different inlet $Hg^0$ concentrations can be predicted by the L-H model.

In the kinetic study of $Hg^0$ photocatalytic oxidation on $TiO_2$ particles by Lee *et al.* (2004), the reaction orders with respect to initial $Hg^0$ concentration (which ranged from 1–10 $\mu$g $m^{-3}$ or 0.005–0.05 $\mu$-mol $m^{-3}$) were reported to be 1.4 for the differential bed reactor (DBR) and 1.1 for the aerosol flow reactor (AFR). They also suggested that the higher value obtained for the DBR might be due to inherent experimental errors. In this work, the fix-bed reactor design is similar to the DBR used by Lee *et al.* (2004). With the inlet $Hg^0$ concentration ranging from 0.19 to 1.28 $\mu$-mol $m^{-3}$ in this study, the value of $K_{Hg}C_{Hg}$ is far less than 1. Thus, equation (8) can be simplified as

$$r = kK_{Hg}C_{Hg} \tag{12}$$

Equation (12) shows that the reaction order with respect to the initial $Hg^0$ concentration is 1, which is representative of a practical sorbent process (Lee *et al.*, 2004). Lee *et al.* (2004) also correlated the overall reaction order with respect to the UV intensity and reported an order of 0.35 for the DBR and 0.39 for the AFR. In this study, the effect of UV intensity was not investigated.

Useful prediction results can be obtained from the L-H model as shown in Fig. 5, which is characterized by a steep rise of $Hg^0$ photocatalytic oxidation rate at inlet concentrations approximately less than 20 $\mu$-mol $m^{-3}$ and subsequent mild increase at higher concentrations. Due to the limitations on the capability of the Hg generation unit and the measurement range of the Hg analyzer,

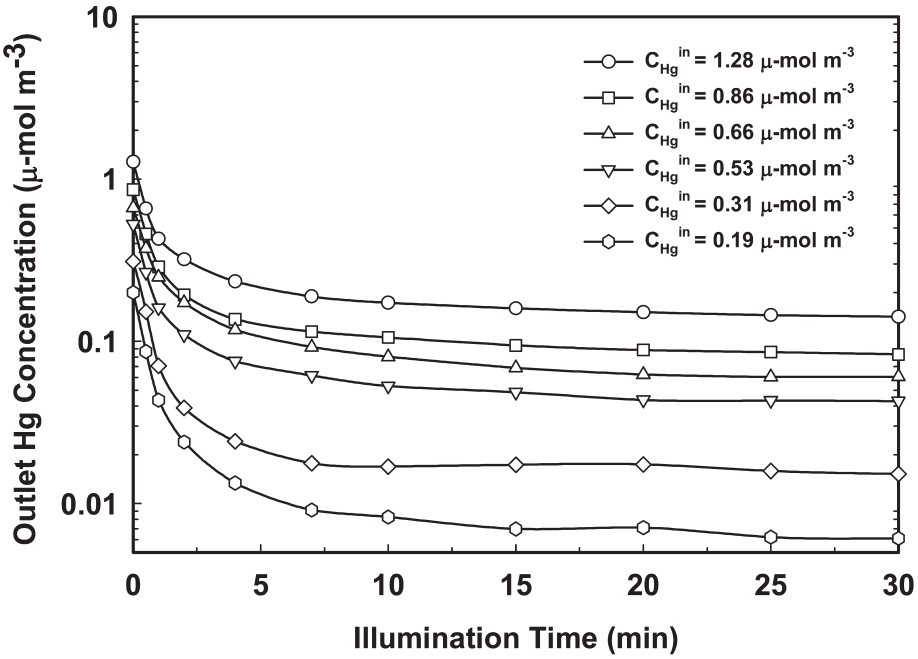


**Figure 3.** Photocatalytic oxidation of $Hg^0$ at different inlet $Hg^0$ concentrations without water vapor.

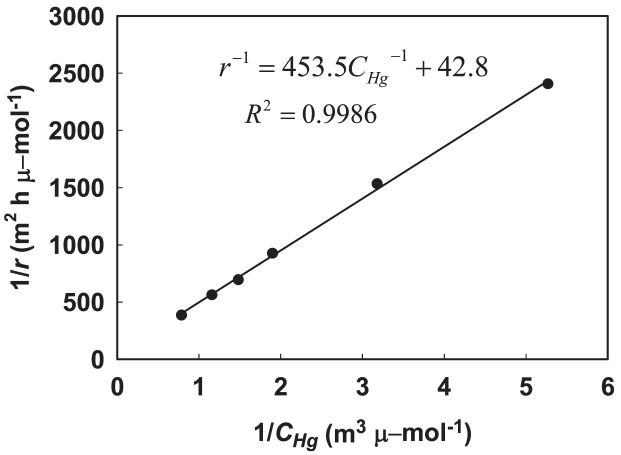


**Figure 4.** The inverse of $Hg^0$ photocatalytic oxidation rate vs. the inverse of inlet $Hg^0$ concentration (without water vapor).

experimental data greater than 20 $\mu$-mol $m^{-3}$ were not available in this study. Further research is needed on validating the L-H feature of $Hg^0$ photocatalytic oxidation in the high concentration range. On the other hand, it should be noted that typical Hg concentrations in coal-fired power plant flue gases are less than 0.05 $\mu$-mol $m^{-3}$ (10 $\mu$g $m^{-3}$) (Pavlish *et al.*, 2003), which locates this process at the very lower end of the steep-rise range. This further demonstrates the great potential of the $SiO_2$–$TiO_2$ nanocomposite for $Hg^0$ removal from emission sources even with much higher $Hg^0$ concentrations.

### *Effect of water vapor*

Water vapor experiments were conducted at a constant inlet $Hg^0$ concentration of 0.66 $\mu$-mol $m^{-3}$ with variations in the water vapor concentration, as shown in Fig. 6. As the water vapor concentration increased from 0 to 0.95 mol $m^{-3}$, the steady-state $Hg^0$ removal efficiency (at 30 min) also decreased from 93 to 24%. This demonstrates a significant inhibitory effect of water vapor on photocatalytic $Hg^0$ oxidation. Experiments were repeated three times at each water vapor concentration level. The average values of $r^{-1}$ vs. $C_w$ at a constant inlet $Hg^0$ concentration are plotted in Fig. 7. The linear relationship between them shows a good match of the experimental data with the L-H model expression in humid air [equation (11)]. The intercept and the slope of the linear plot give the L-H rate constant $k = 0.031$ $\mu$-mol $m^{-2}$ $h^{-1}$ and the Langmuir adsorption constant of water $K_w = 4.39$ $m^3$ $mol^{-1}$. The previously obtained $K_{Hg}$ (0.094 $m^3$ $\mu$-$mol^{-1}$ or $9.4 \times 10^4$ $m^3$ $mol^{-1}$) is four orders of magnitude larger than $K_w$, which indicates that the adsorption ability of the $SiO_2$–$TiO_2$ nanocomposite is much greater for $Hg^0$ than for water vapor. However, water vapor plays a very im-

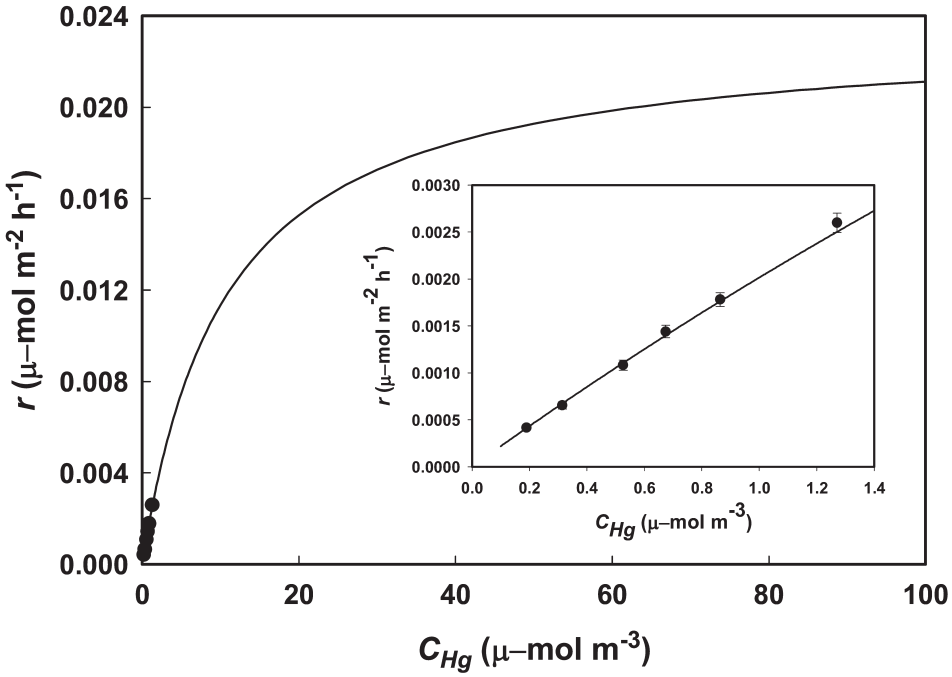


**Figure 5.** Rate of $Hg^0$ photocatalytic oxidation vs. inlet $Hg^0$ concentration without water vapor (solid circles: experimental data; solid line: L-H model).

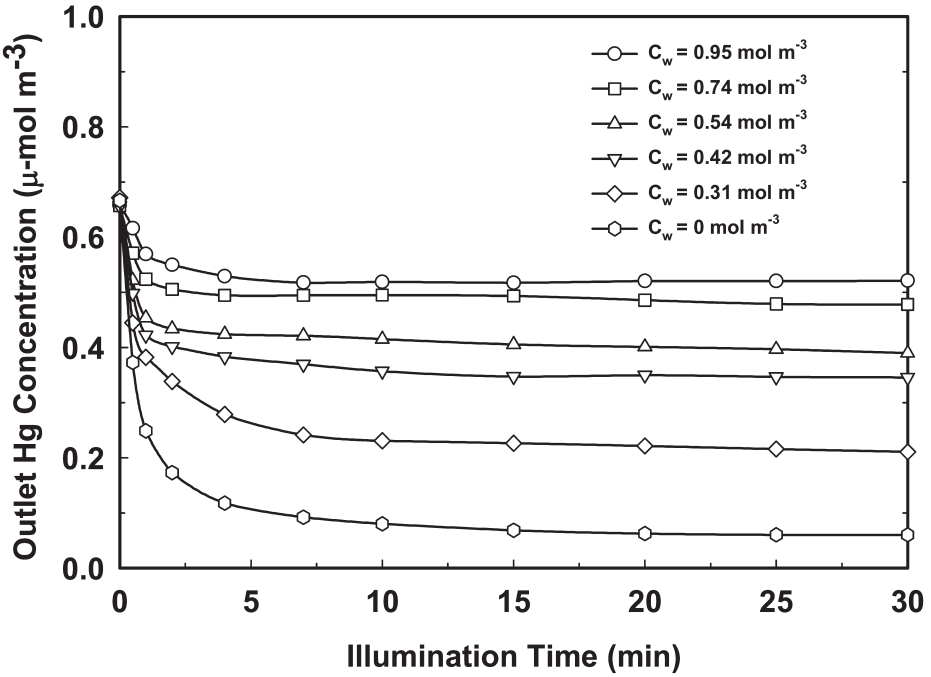


**Figure 6.** Photocatalytic oxidation of $Hg^0$ at a constant inlet $Hg^0$ concentration of 0.66 $\mu$-mol $m^{-3}$ with variation in water vapor concentration.

portant role in $Hg^0$ removal because in the flue gas $Hg^0$ concentration is at such trace levels (seven to eight orders of magnitude smaller) compared to that of water vapor.

Now that all the kinetic parameters have been estimated, the L-H model can be used to predict the rate of $Hg^0$ photocatalytic oxidation at any level of inlet $Hg^0$ concentration and water vapor concentration. Figure 8 compares the experimental data of the $Hg^0$ photocatalytic oxidation rate with L-H model predictions in humid air. For the six experimental conditions shown in Fig. 8, the deviations of the experimental data from the L-H model predictions are less than 15%, which are within an allowable range of experimental error. This result once again verifies the L-H nature of $Hg^0$ photocatalytic oxidation by the $SiO_2$-$TiO_2$ nanocomposite, and suggests that it is appropriate to apply the L-H model to predict the photocatalytic reaction rate. Using the L-H model, the rate of $Hg^0$ oxidation by $SiO_2$–$TiO_2$ under coal combustion flue gas conditions can be predicted. At an inlet $Hg^0$ concentration of 0.05 $\mu$-mol $m^{-3}$ (10 Mg $m^{-3}$) and a water vapor concentration of 10 vol%, the reaction rate is calculated to be $7.7 \times 10^{-6}$ $\mu$-mol $m^{-2}$ $h^{-1}$ and the $Hg^0$ removal efficiency is around 7% in the current system ($Q$ = 0.12 $m^3$ $h^{-1}$ and $A_e$ = 52.5 $m^2$ or 2.5 g of pellets used). However, a 95% removal efficiency can be achieved by increasing $A_e$ by 14-fold (using 35 g of pellets or 56 mm bed height), which is practically applicable in a bench-scale reactor like the one used in this work. In addition, increasing the UV power level can be another option to reduce the required amount of catalysts as the reaction rate is proportional to the UV intensity (Lee *et al*., 2004).

It is generally believed (Kim and Hong, 2002; Pitoniak *et al*., 2003; Raillard *et al*., 2004; Rodriguez *et al*., 2004; Shang *et al*., 2002) that the inhibitory effect of water vapor on photocatalytic reactions at relatively high

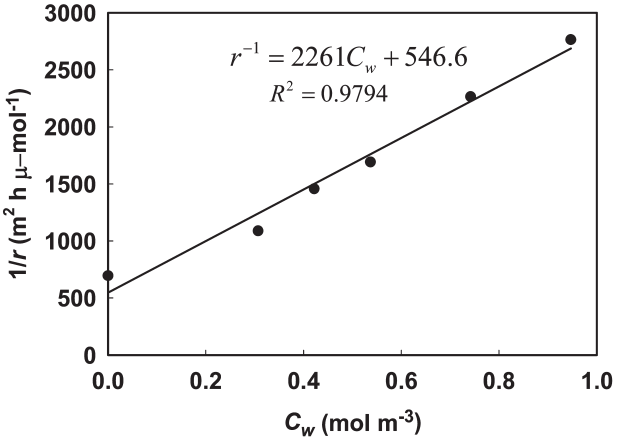


**Figure 7.** The inverse of $Hg^0$ photocatalytic oxidation rate vs. water vapor concentration at a constant inlet $Hg^0$ concentration of 0.66 $\mu$-mol $m^{-3}$.

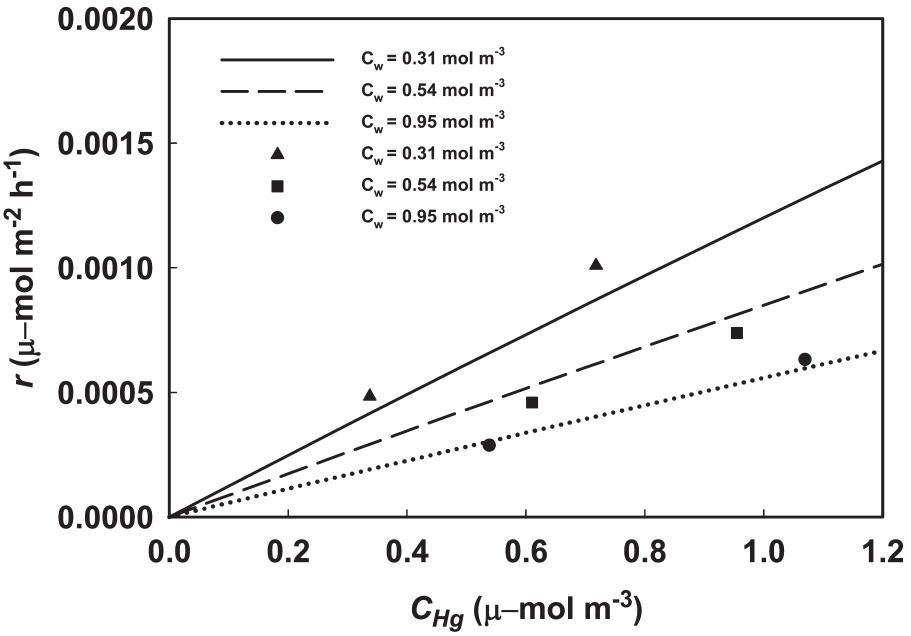


**Figure 8.** Rate of $Hg^0$ photocatalytic oxidation vs. inlet $Hg^0$ concentration at different water vapor concentrations (markers: experimental data; lines: L-H model).

water vapor concentrations is due to the competition between water vapor and the pollutants at the $TiO_2$ surface, that is, a high concentration of water vapor blocks the adsorption sites from pollutants. Unlike the mechanistic model developed by Rodríguez *et al.* (2004), where water vapor promoted $Hg^0$ capture by *in situ*-generated $TiO_2$ particles at low water vapor concentrations (<2,000 $ppm_v$ or 0.0815 mol $m^{-3}$ at 25°C), the $Hg^0$ capture rate by the $SiO_2$–$TiO_2$ nanocomposite in this study reached maximum in dry air and decreased as the water vapor concentration increased. An explanation for the highest photocatalytic oxidation rate without water vapor may be related to the silanol (Si—OH) groups on the surface of the $SiO_2$–$TiO_2$ nanocomposite. The sol–gel reactions are performed in water/alcohol systems that cannot avoid the reverse reactions during the sol–gel process, that is, hydrolysis and alcoholysis for silanol formation (Yang and Chen, 2005). Yang and Chen (2005) reported that a $SiO_2$ nanolayer around $TiO_2$ nanocrystals can enhance the efficiency of photocatalysis because the transfer of electrons to the silica sites and the hole scavenging by the hydroxides at the $TiO_2$–$SiO_2$ interface prevent the electrons and holes from recombination. In the $SiO_2$–$TiO_2$ nanocomposite produced in this work, the hydroxyl groups from silanols may act as traps for the holes generated by $TiO_2$ under UV irradiation, and thus, an adequate number of hydroxyl radicals may be produced resulting in photocatalytic oxidation of $Hg^0$ even in the absence of water vapor. Similar findings were reported by Kim and Hong (2002) that photodegradation of methanol by $TiO_2$ reached the highest rate at considerably low water concentrations, which was explained due to the production of hydroxyl radicals from hydroxyl groups of methanol itself. In this manner, hydroxyl radicals generated from water molecules might be insignificant, and addition of water vapor may only prohibit $Hg^0$ photocatalytic oxidation by blocking the $Hg^0$ adsorption sites on the surface of the $SiO_2$–$TiO_2$ nanocomposite. In the system of Rodríguez *et al.* (2004), $Hg^0$ photocatalytic oxidation rate increased with water vapor at low water vapor concentrations, which may be because water vapor was the only source for hydroxyl radical production. Comparisons between this study and that by Rodríguez *et al.* (2004) suggest that hydrophilic adsorbents (such as $SiO_2$–$TiO_2$ nanocomposite) may have better performance in $Hg^0$ removal at dry or very low humidity environment, and on the other hand, hydrophobic materials (such as $TiO_2$ nanoparticles) may yield a larger $Hg^0$ removal rate as the humidity increases. However, the performance of both types of materials will be inhibited at very high water vapor concentrations.

## CONCLUSIONS

The kinetics of $Hg^0$ photocatalytic oxidation on a $SiO_2$–$TiO_2$ nanocomposite under UV irradiation was studied through experiments in a fixed-bed reactor. An

L-H model was used to analyze the kinetic data. Good agreement between the experimental data and the L-H model was demonstrated, indicating the validity of using the L-H model to describe the kinetics of $Hg^0$ photocatalytic oxidation. Model predictions demonstrate a great potential of the $SiO_2$–$TiO_2$ nanocomposite for $Hg^0$ removal even at very high $Hg^0$ concentrations. The rate of photocatalytic $Hg^0$ oxidation increased when the inlet $Hg^0$ concentration increased, and it reached a maximum value in the absence of water vapor. The addition of water vapor was found to inhibit $Hg^0$ photocatalytic oxidation, which may be explained by the competitive adsorption of water vapor with $Hg^0$ on the $TiO_2$ surface.

## ACKNOWLEDGMENTS

This study was partially supported by the STAR program of the U.S. EPA under Grant No. R-82960201. The authors are thankful to Patrick Murphy for helping with the experiments.

## REFERENCES

BROWN, T.D., SMITH, D.N., HARGIS, R.A., and O'DOWD, W.J. (1999). Mercury measurement and its control: What we know, have learned, and need to further investigate. *J. Air Waste Manage. Assoc.* **49**(6), 628.

CANELA, M.C., ALBERICI, R.M., and JARDIM, W.F. (1998). Gas-phase destruction of H2S using $TiO_2$/UV-VIS. *J. Photochem. Photobio. A: Chem.* **112**(1), 73.

CHEN, S., ROSTAM-ABADI, M., and CHANG, R. (1996). Mercury removal from combustion flue gas by activated carbon injection: mass transfer effects. *Prepr. Pap.-Am. Chem. Soc., Div. Fuel Chem.* **41**(1), 442.

EDWARDS, J.R., SRIVASTAVA, R.K., and KILGROE, J.D. (2001). A study of gas-phase mercury speciation using detailed chemical kinetics. *J. Air Waste Manage. Assoc.* **51**(6), 869.

FLORA, J.R.V., VIDIC, R.D., LIU, W., and THURNAU, R.C. (1998). Modeling powdered activated carbon injection for the uptake of elemental mercury vapors. *J. Air Waste Manage. Assoc.* **48,** 1051.

KIM, S.B., and HONG, S.C. (2002). Kinetic study for photocatalytic degradation of volatile organic compounds in air using thin film $TiO_2$ photocatalyst. *Appl. Catal. B-Environ.* **35**(4), 305.

LEE, T.G., HEDRICK, E., and BISWAS, P. (2001). Comparison of mercury capture efficiencies of three different in-situ generated sorbent. *AICHE J.* **47,** 954.

LEE, T.G., BISWAS, P., and HEDRICK, E. (2004). Overall kinetics of heterogeneous elemental mercury reactions on $TiO_2$ sorbent particles with UV irradiation. *Ind. Eng. Chem. Res.* **43**(6), 1411.

MESEROLE, F.B., RICHARDSON, C.F., MILLER, S.D., SEARCY, K., and CHANG, R. (2000). Estimated the costs of electric utility mercury control using sorbent injection. *Proceedings of the Air and Waste Management Association 93rd Annual Meeting,* Salt Lake City, UT, Paper AE I-144.

NIKSA, S., HELBLE, J.J., and FUJIWARA, N. (2001). Kinetic modeling of homogeneous mercury oxidation: The importance of NO and $H_2O$ in predicting oxidation in coal-derived systems. *Environ. Sci. Technol.* **35**(18), 3701.

OBEE, T.N. (1996). Photooxidation of sub-parts-per-million toluene and formaldehyde levels an titania using a glass-plate reactor. *Environ. Sci. Technol.* **30**(12), 3578.

OBEE, T.N., and HAY, S.O. (1997). Effects of moisture and temperature on the photooxidation of ethylene on Titania. *Environ. Sci. Technol.* **31**(7), 2034.

PAVLISH, J.H., SONDREAL, E.A., MANN, M.D., OLSON, E.S., GALBREATH, K.C., LAUDAL, D.L., and BENSON, S.A. (2003). Status review of mercury control options for coal-fired power plants. *Fuel Process. Technol.* **82**(2–3), 89.

PITONIAK, E., WU, C.Y., LONDEREE, D., MAZYCK, D., BONZONGO, J.C., POWERS, K., and SIGMUND, W. (2003). Nanostructured silica-gel doped with $TiO_2$ for mercury vapor control. *J. Nanopart. Res.* **5**(3–4), 281.

PITONIAK, E., WU, C.Y., MAZYCK, D.W., POWERS, K.W., and SIGMUND, W. (2005). Adsorption enhancement mechanisms of silica–titania nanocomposites for elemental mercury vapor removal. *Environ. Sci. Technol.* **39**(5), 1269.

RAILLARD, C., HEQUET, V., LE CLOIREC, P., and LEGRAND, J. (2004). Kinetic study of ketones photocatalytic oxidation in gas phase using $TiO_2$-containing paper: Effect of water vapor. *J. Photochem. Photobio. A: Chem.* **163**(3), 425.

RODRIGUEZ, S., ALMQUIST, C., LEE, T.G., FURUUCHI, M., HEDRICK, E., and BISWAS, P. (2004). A mechanistic model for mercury capture with in situ-generated titania particles: Role of water vapor. *J. Air Waste Manage. Assoc.* **54**(2), 149.

ROSTAM-ABADI, M., CHEN, S.G., HSI, H.-C., ROOD, M., CHANG, R., CAREY, T.R., HARGROVE, B., RICHARDSON, C., ROSENHOOVER, W., and MESEROLE, F. (1997). Novel vapor phase mercury sorbents. *Proceedings of the EPRI-DOE-EPA Combined Utility Air Pollutant Control,* Washington, DC, Aug 25–29, 1997, TR-108683-V3.

SHANG, J., DU, Y.G., and XU, Z.L. (2002). Photocatalytic oxidation of heptane in the gas-phase over $TiO_2$. *Chemosphere* **46**(1), 93.

SHOLUPOV, S., POGAREV, S., RYZHOV, V., MASHYANOV, N., and STROGANOV, A. (2004). Zeeman atomic absorption spectrometer RA-915+ for direct determination of mer-

cury in air and complex matrix samples. *Fuel Process. Technol.* **85**(6–7), 473.

SON, H.S., LEE, S.J., CHO, I.H., and ZOH, K.D. (2004). Kinetics and mechanism of TNT degradation in $TiO_2$ photocatalysis. *Chemosphere* **57**(4), 309.

U.S. ENVIRONMENTAL PROTECTION AGENCY. (1997). Mercury Study Report to Congress. EPA-452/R-97-003.

U.S. ENVIRONMENTAL PROTECTION AGENCY. (2005). Standards of performance for new and existing stationary sources: Electric utility steam generating units: Final rule. *Fed. Reg.* **70,** 28606.

WU, C.Y., LEE, T.G., TYREE, G., ARAR, E., and BISWAS, P. (1998). Capture of mercury in combustion systems by in-situ generated titania particles with UV irradiation. *Environ. Eng. Sci.* **15**(2), 137.

YANG, C.S., and CHEN, C.J. (2005). Synthesis and characterization of silica-capped titania nanorods: An enhanced photocatalyst. *Appl. Catal. A-General* **294**(1), 40.